APPROXIMATE CONTROLLER DESIGN FOR SINGULARLY PERTURBED AIRCRAFT

A Thesis by

Joseph E. Graziosi

Bachelor of Science, Wichita State University, 2009

Submitted to the Department of Electrical Engineering and Computer Science
and the faculty of the Graduate School
of Wichita State University
in partial fulfillment of
the requirements for the degree of Master of Science

May 2014

APPROXIMATE CONTROLLER DESIGN FOR SINGULARLY PERTURBED AIRCRAFT

The following faculty members have examined the final copy of this thesis for form and content, and recommended that it be accepted in partial fulfillment of the requirement for the degree of Master of Science, with a major in Electrical Engineering.

_____
John Watkins, Committee Chair

_____
M. Edwin Sawan, Committee Member

_____
Brian Driessen, Committee Member

DEDICATION

To my God, my wife and children, and my dear friends

ACKNOWLEDGEMENTS

I would like to thank my advisors, Dr. Sawan and Dr. Watkins, for their guidance and influence on the completion of my thesis and for their patience in accommodating my work schedule. I also thank my current and past supervisors and co-workers for their support. Lastly, and most of all, I thank my wife and children for their love and understanding through the countless hours and late nights spent on my studies these past years.

ABSTRACT

The purpose of this thesis was to extend the quasi-steady-state approximation and matrix block diagonalization methods utilized in the work of Shim and Sawan [1]. These authors showed that an approximate controller solution could be developed by relocating only the slow poles for two-time-scale aircraft dynamics. In addition, they showed that the difference between approximate solutions and exact solutions was bounded within limits as $O(\varepsilon)$ and $O(\varepsilon^2)$. This technique was successfully applied to the lateral dynamics of the de Haviland Canada DHC-2 Beaver aircraft.

In this thesis, the same technique was applied to the NASA F-8 aircraft dynamics in order to show that the method is not unique to the Beaver and can be applied to other aircraft models. It also extended the method to consider the singularly perturbed stochastic system and showed that a finite solution to the Lyapunov equation existed as a result of the stability.

TABLE OF CONTENTS

Chapter Page

1. INTRODUCTION 1

2. METHODOLOGY 3

2.1 Singular Perturbation Method 3
2.2 Block Diagonalization 4
2.3 Quasi-Steady State 6
2.4 Stochastic Condition 8

3. AIRCRAFT APPLICATIONS 10

4. SIMULATION 15

4.1 Stochastic Condition 19

5. CONCLUSION AND FUTURE WORK 21

6. REFERENCES 23

LIST OF FIGURES

Figure Page

2-1. Typical Stochastic System Block Diagram. 8

4-1. Exact Solution at -0.0050. 15

4-2. Exact Solution at -0.0100 15

4-3. Uncorrected Solution at -0.0050 16

4-4. Uncorrected Solution at -0.0100 16

4-5. Corrected Solution at -0.0050 17

4-6. Corrected Solution at -0.0100 17

CHAPTER 1

INTRODUCTION

A myriad of methods, tools and techniques are available to controls engineers to assist them in modeling, analyzing, and designing systems. Yet, as with most goals in both academia and industry, the ability to find solutions in a minimal amount of time is desired. Often times in industry, practical problems arise and need to be answered in a minimal amount of time. A problem may require only a simple approximate answer or "back of the envelope" calculation instead of a complex analysis, in order to allow other work to proceed or to determine if a particular design path is acceptable. In these cases, an approximation or verification may be all that is required. These types of circumstances where only a validation is required allow minimal impact on project schedules and program costs.

In controls engineering applications, to achieve these "quick-look" solutions, reducing system sizes and orders can be beneficial. However, this can also run the risk of reducing accuracy. Having techniques that can do both is clearly advantageous.

By taking a dynamic system and separating its eigenvalues into two distinct groups of fast and slow variables means to convert it to a two-time-scale system [1]. But even at this stage, it is still challenging to compute a solution. In order to further simplify the process, two techniques that reduce system sizes and orders are utilized: matrix block diagonalization and quasi-steady-state approximation [2]. When both processes are used together, this is called the singular perturbation method.

In conjunction with the above techniques, at times it is prudent and necessary to consider the effects of external forces. Even though these forces are unpredictable, it is

still important to understand their impact. Methods used for solving stochastic systems are employed to show stability that is still preserved.

As shown in this thesis, utilizing the methods of slow pole relocation along with considering stochastic behavior provides a useful and reliable methodology. This will allow expedient insight into the effects of design changes without a lengthy and complex analysis.

CHAPTER 2

METHODOLOGY

2.1 Singular Perturbation Method

The singular perturbation technique provides a way to simplify a system model through order reduction and size [3], while at the same time retaining accuracy. This is accomplished through the consideration of parameters that are normally neglected in simplified models. These typically neglected parameters are accounted for as a scalar, represented by the variable ε. In the context of a state-space model, this can be represented as

$$\dot{x} = f(x, z, \varepsilon, t),\ x(t_0) = x_0,\ x \in R^n \tag{2.1}$$

$$\varepsilon\dot{z} = g(x, z, \varepsilon, t),\ z(t_0) = z_0,\ z \in R^m \tag{2.2}$$

where the derivatives are with respect to time, and f and g are continuously differentiable functions of $x, z, \varepsilon, and\ t$. As stated above, order reduction is desired and is achieved by conversion to a parameter perturbation known as “singular.” If ε = 0, then the state space dimension of equations (2.1) and (2.2) will be reduced to n instead of n + m, from which proceeds the following the algebraic equation:

$$0 = g(\bar{x}, \bar{z}, 0, t) \tag{2.3a}$$

where the bar above the functions indicates the variables of a system where ε = 0. It can be stated that if equation (2.3a) has distinct real roots such that

$$\bar{z} = \overline{\Phi_i}(\bar{x}, t),\ for\ i = 1, 2, \ldots, k, \tag{2.3b}$$

then equations (2.1) and (2.2) are considered to be in standard form.

A two-time-scale system occurs when a system’s eigenvalues are separated into slow and fast groups. The two-time-scale model for a time-invariant system is given as

$$\dot{x} = A_{11}x + A_{12}z + B_1u,\ x(t_0) = x^0 \tag{2.4}$$

$$\varepsilon\dot{z} = A_{21}x + A_{22}z + B_2u,\ z(t_0) = z^0 \tag{2.5}$$

where x and z are n- and m-dimensional state vectors, respectively, and the A matrices are of appropriate dimensionality. In addition, A_{22} must be non-singular. In order for equations (2.4) and (2.5) to have a two-time-scale property, the following must be true:

$$0 < |\lambda_{s1}| < |\lambda_{s2}| \dots |\lambda_{sn}| < |\lambda_{f1}| < |\lambda_{f2}| \dots |\lambda_{fm}| < \left|\frac{2}{\Delta}\right| \tag{2.6}$$

where λ represents the eigenvalues of the system and

$$\varepsilon = |\lambda_{sn}|/|\lambda_{f1}| \ll 1 \tag{2.7}$$

From this, it follows that the following inequality holds:

$$|\lambda_{\max}\ \ (A_s)| \ll |\lambda_{min}(A_{f)}| \tag{2.8}$$

Consequently, if the norm of the invertible matrices are used, then the following is true [1]:

$$|A_f|^{-1} \ll |A_s|^{-1} \tag{2.9a}$$

With equations (2.4) to (2.9a) providing the basis for the two-time-scale system, the model can be written as

$$\begin{bmatrix} \dot{x}(t) \\ \varepsilon\dot{z}(t) \end{bmatrix} = \begin{bmatrix} A_{11} & A_{12} \\ A_{21} & A_{22} \end{bmatrix} \begin{bmatrix} x(t) \\ z(t) \end{bmatrix} + \begin{bmatrix} B_1 \\ B_2 \end{bmatrix} u(t) \tag{2.9b}$$

The process of decoupling the system into its fast and slow constituents will be discussed in the next section.

2.2 Block Diagonalization

Block diagonalization is a transformation method by which two-time-scale systems are separated into fast and slow subsystems. Decoupling allows them to be addressed separately. First, the system can be rewritten as [4]

$$x_s(\tau) = (I_s - ML)x(\tau) - Mz(\tau) \tag{2.10}$$

$$z_f(\tau) = Lx(\tau) + I_f z(\tau) \tag{2.11}$$

From here, equations (2.1) and (2.2) can be expressed as slow and fast subsystems [5], respectively:

$$\begin{bmatrix} \dot{x_s}(t) \\ \dot{z_f}(t) \end{bmatrix} = \begin{bmatrix} A_s & 0 \\ 0 & A_f \end{bmatrix} \begin{bmatrix} x_s(t) \\ z_f(t) \end{bmatrix} + \begin{bmatrix} B_s \\ B_f \end{bmatrix} u(t) \tag{2.12}$$

where

$$A_s = A_{11} - A_{12}L, \quad A_f = A_{22} + LA_{22} \tag{2.13}$$

$$B_s = B_1 - MB_2 - MLB_1, \quad B_f = B_2 + LB_1 \tag{2.14}$$

L and M as solutions to the algebraic Riccatti equation (ARE) are as follows:

$$LA_{11} + A_{21} - LA_{12}L - A_{22}L = 0 \tag{2.15}$$

$$A_{11}M - A_{12}LM - MA_{22} - MLA_{12} + A_{12} = 0 \tag{2.16}$$

The initial conditions for L and M are as follows:

$$L_0 = A_{22}^{-1}A_{21}, \quad M_0 = A_{12}A_{22}^{-1} \tag{2.17}$$

$$A_0 = A_{11} - A_{12}L_0, \quad B_0 = B_1 - M_0B_2 \tag{2.18}$$

When

$$\left\|A_{22}^{-1}\right\| \ll \{3(\|A_0\| + \|A_{12}\| \cdot \|L_0\|)\}^{-1} \tag{2.19}$$

then L_k and M_k sequences are:

$$L_{k+1} = A_{22}^{-1}(A_{21} + L_kA_{11} - L_kA_{12}L_k) \tag{2.20}$$

$$M_{k+1} = (A_{11} + A_{12} - A_{12}L_kM_k - M_kL_kA_{12})A_{22}^{-1} \tag{2.21}$$

From the work of Kokotovic [4], it can be shown that a system exhibits the two-time-scale property, if the following holds:

$$\|A_{22}^{-1}\| \ll \{\|A_0\| + \|A_{12}\| \cdot \|L_0\|\}^{-1} \tag{2.22}$$

From here, the approximate expressions for x and z can be obtained, respectively, as

$$x(t) = x_0(t) + A_{12}A_{22}^{-1}z_0(t) + O(u) \tag{2.23}$$

$$z(t) = A_{22}^{-1}A_{21}x_0(t) + z_0(t) + O(u) \tag{2.24}$$

where x_{s0} and x_{f0} are obtained from simplified subsystems [1] as

$$\begin{bmatrix} \dot{x(t)} \\ \dot{z(t)} \end{bmatrix} = \begin{bmatrix} A_0 & 0 \\ 0 & A_{22} \end{bmatrix} \begin{bmatrix} x_0(t) \\ z_0(t) \end{bmatrix} + \begin{bmatrix} B_0 \\ B_2 \end{bmatrix} u_0(t) \tag{2.25}$$

2.3 Quasi-Steady State

The quasi-steady-state approach is a method by which fast subsystems are assumed to have reached a steady state. Beginning with the standard form, the system becomes

$$\begin{bmatrix} \dot{\overline{x}}(t) \\ 0 \end{bmatrix} = \begin{bmatrix} A_{11} & A_{12} \\ A_{21} & A_{22} \end{bmatrix} \begin{bmatrix} \overline{x}(t) \\ \overline{z}(t) \end{bmatrix} + \begin{bmatrix} B_1 \\ B_2 \end{bmatrix} u_0(t) \tag{2.26}$$

where the system reduces to

$$\dot{\overline{x}}(t) = A_0\overline{x}(t), \tag{2.27a}$$

$$\overline{z}(t) = A_{22}^{-1}(A_{21}\overline{x}(t) + B_2\overline{u}(t)) \tag{2.27b}$$

where the bar above the functions indicates the quasi-steady state. To visualize this, since the x term (slow subsystem) is varying slowly in comparison to the fast subsystem, the z term has decayed to the point where its derivative with respect to time is zero. Therefore, $x_0,\ A_{22}^{-1}A_{21}x_0$ is a quasi-steady state of x. For the slow portions of x(t) and z(t), approximations to achieve O(ε) by letting ε = 0 will set the $\dot{z}$ term of (1.10) to zero. Then, substituting equation (2.28) into equation (2.27) results in

$$\dot{x_s}(t) = A_0 x_s(t) + B_0 u_s(t),\ for\ x_s(0) = x_{s0} \tag{2.28}$$

where $A_0$and B_0 are the same as in the initial condition of equation (2.18), and $\overline{x} = x_s$, $\overline{u} = u_s$, $\overline{y}$ are the slow portions of equations (2.14) and (2.15). Additionally, for the fast modes, the slow variables are assumed to be constant. The fast subsystem of equation (2.9b) then can be defined as

$$z_f(\tau) = A_{22} z_f(\tau) + B_2 u_f(\tau), \quad z_f(0) = z_0 - \bar{z}_0(0) \tag{2.29}$$

where

$$z_f = z - \overline{z}, \tag{2.30a}$$

$$u_f = u - u_s \tag{2.30b}$$

The term O(ε) is an order of magnitude approximation for ε corresponding to a very small value established by determining the ratio of the smallest eigenvalue of the fast subsystem to the largest eigenvalue of the slow subsystem.

Separately designed feedback controls for the slow and fast subsystems are, respectively,

$$\mathrm{u_s} = \mathrm{G_0 x_s} \tag{2.31}$$

$$\mathrm{u_f} = \mathrm{G_2 z_f} \tag{2.32}$$

where G_o and G_2 are the feedbacks from pole placement for the slow and fast systems, respectively. For the uncorrected solution, the O(ε) term is a first-order magnitude of error value that the solution will satisfy the following:

$$\lambda_{\mathrm{desired}} = \lambda(\mathrm{A_0 + B_0 G_0}) + \mathrm{O}(\varepsilon) \tag{2.33}$$

where λ is the eigenvalue of the closed loop plant [6].

For the corrected solution, the $O(\varepsilon^2)$ term is a second-order magnitude of error value that the solution will satisfy the following:

$$\lambda_{\text{desired}} = \lambda(A_{sc} + B_{sc}G_{sc}) + O(\varepsilon^2) \tag{2.34}$$

where λ is the eigenvalue of the closed-loop plant [3].

2.4 Stochastic Condition

External influences must be considered to ensure that the modeled results reflect the practical real-world environments. For aircraft, these influences are typically characterized as forces or disturbances during flight, i.e., wind, gusts, turbulence, etc. Due to the unpredictable nature of these influences, they must be treated as random variables. Therefore, the stochastic process is utilized to account for these influences and determine their impact to the model.

The method used to solve for these stochastic conditions considers the disturbances as a white Gaussian noise with zero mean. A typical stochastic system block diagram is shown in Figure 2-1.

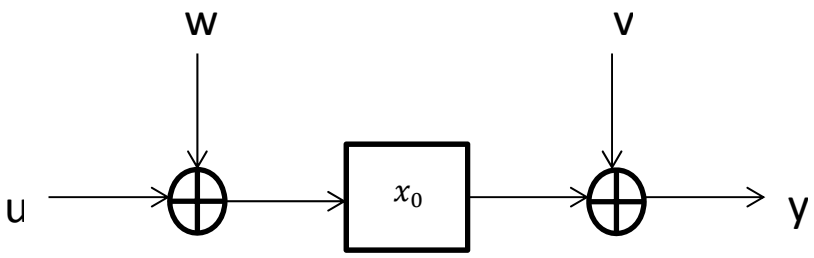

Figure 2-1. Typical Stochastic System Block Diagram.

Here, x_0 is the random variable, u is the input, w is the process noise, and v is the measurement noise. Since the noise is treated as Gaussian, the process noise w and measurement noise v are uncorrelated and therefore independent.

For the continuous time system, the model for Figure 2-1 can be represented as

$$\dot{x} = Ax + Bu + Gw \tag{2.35}$$

$$y = Cx + Hv \tag{2.36}$$

To address the non-deterministic property of the system, the mean of the response of the stochastic system is computed from the following:

$$\dot{m}_x = Am_x \tag{2.37}$$

$$m_x = \Phi(t)m_x(0) \tag{2.38}$$

where the characteristic equation is

$$\Phi(t) = e^{At} = \mathcal{L}^{-1}\{(SI - A)^{-1} \tag{2.39}$$

Finally, the steady-state covariance matrix is computed using the algebraic Lyapunov equation [7]:

$$PA^T + AP + Q = 0 \tag{2.40}$$

where

$$Q = FQF^T \tag{2.41}$$

$$F = F_1 - A_{12}A_{22}^{-1}F_2 \tag{2.42}$$

A positive definite matrix of the solution will be achieved as a result of the system stability.

CHAPTER 3

AIRCRAFT APPLICATIONS

Shim and Sawan [1] utilized the aforementioned techniques and applied them to the de Haviland Canada DHC-2 Beaver aircraft. This single-engine, high–wing, all-metal aircraft is manufactured by de Havilland Aircraft of Canada (now under Bombardier Aerospace). Some basic specifications of the Beaver are as follows [8]:

Fuselage length: 9.22 m

Wing span: 14.63 m

Wing area: 23.23 m^2

Mean aerodynamic chord: 1.5875 m

Wing sweep: 0 deg

Wing dihedral: 1 deg

Maximum take-off weight: 22,800 N

Empty weight: 14,970 N

Engine: Pratt and Whitney Wasp Jr. R-985

Maximum power: 450 Hp at n = 2300 RPM, pressure altitude = 26 in. Hg

Propeller: Hamilton Standard, two-bladed metal regulator propeller

Diameter of propeller: 2.59 m

Lateral dynamics were utilized in this study, the. Using an epsilon value of 0.0424, the open-loop poles—two slow and two fast poles—were calculated. Only the slow poles were relocated to an arbitrary value (but still on the left-half plane).

The simulation showed that the uncorrected and corrected solutions closely followed the exact solutions, thereby indicating that not only robustness is maintained

but this method proves that it can reduce computational complexity and still be viable enough for implementation in practical applications.

To verify that the above computational techniques are not unique to a particular set of values or that they produce solutions only for the numerical quantities associated with the physical characteristics of the de Havilland Beaver, these same computational methods were applied to the NASA F-8 digital fly-by-wire (DFBW) aircraft.

The F-8 aircraft experiment was conducted jointly by the Dryden Flight Research Center and the Langley Research Center. The goal of the program was to investigate and advance the technology for DFBW systems in aircraft [7]. During this effort, much information concerning control systems and control laws was published. With this vast amount of accessible information pertaining to a particular control system, the application of techniques to the F-8 aircraft that were used in this thesis makes it advantageous, since it allows the results to be readily understood and verifiable against available data. Some basic specifications of the F-8 Aircraft are as follows:

Manufacturer: LTV Aerospace, Dallas, Texas

Powerplant: Pratt and Whitney J57 turbojet

Wingspan: 35 feet 2 inches (350 square feet)

Overall length: 54 feet 6 inches

Overall height: 15 feet 9 inches

Maximum speed: > 1,000 mph

The longitudinal dynamics utilized for this exercise were based on the following flight conditions [7]:

Altitude: 20,000 ft

Speed: Mach 0.6 (620 ft/sec)

Angle of attack (AOA): 0.078 rad.

The longitudinal dynamics of the F8 aircraft utilized for this exercise are as follows [9]:

$$\mathrm{A} = \begin{bmatrix} -0.0150 & -0.0519 & -0.0226 & 0 \\ 0 & 0 & 0 & 1.0000 \\ -0.1178 & 0 & -0.8400 & 1.0000 \\ 0.0310 & 0 & -4.8000 & -0.4900 \end{bmatrix} \tag{3.1}$$

$$\mathrm{B} = \begin{bmatrix} -0.0018 \\ 0 \\ -0.1100 \\ -8.7000 \end{bmatrix} \tag{3.2}$$

$$\mathrm{C} = \begin{bmatrix} 1 & 0 & 0 & 0 \\ 0 & 1 & 0 & 0 \\ 0 & 0 & 1 & 0 \\ 0 & 0 & 0 & 1 \end{bmatrix} \tag{3.3}$$

where the state variables are as follows:

v = velocity

α = angle of attack (rad)

q = pitch rate (rad/sec)

θ = pitch angle (rad)

The input variable is as follows:

Δ = stabilator deflection (rad)

When the above system is converted to the two-time-scale singularly perturbed form, the following results:

$$\mathrm{A}_{11} = \begin{bmatrix} -0.195378 & -0.676469 \\ 1.478265 & 0 \end{bmatrix} \tag{3.4}$$

$$\mathrm{A}_{12} = \begin{bmatrix} -0.917160 & 0.109033 \\ 0 & 0 \end{bmatrix} \tag{3.5}$$

$$\mathrm{A}_{21} = \begin{bmatrix} -0.051601 & 0 \\ 0.013579 & 0 \end{bmatrix} \tag{3.6}$$

$$\mathrm{A}_{22} = \begin{bmatrix} -0.367954 & 0.43804 \\ -2.102596 & -0.21464 \end{bmatrix} \tag{3.7}$$

$$B_1 = \begin{bmatrix} -0.023109 \\ -16.945030 \end{bmatrix} \tag{3.8}$$

$$B_2 = \begin{bmatrix} -0.048184 \\ -3.810954 \end{bmatrix} \tag{3.9}$$

$$C_1 = \begin{bmatrix} 0 & 1 \\ 0 & 0 \end{bmatrix} \tag{3.10}$$

$$C_2 = \begin{bmatrix} 0.921022 & -0.161179 \\ 0 & 1 \end{bmatrix} \tag{3.11}$$

The open-loop poles of the original system are

$$\text{-0.6656±2.1821i} \tag{3.12}$$

$$\text{-0.0069±0.0765i} \tag{3.13}$$

Applying the techniques of Shim and Sawan [1], only the slow poles were relocated here to arbitrary values of –0.0050 ± 0.0765i and –0.0100 ± 0.0765i . It should be noted that these arbitrary values are only theoretical values to demonstrate the effect of moving the slow poles in this thesis. These values chosen do not necessarily represent a practical solution for optimal performance of this system. Using this new pole location, a feedback gain was generated for both the uncorrected and corrected solutions. Both of these gains were then individually fed back into the original system.

For the uncorrected solution,

$$\dot{x} = (A - BG_u)x \tag{3.14}$$

where Gu is the gain calculated from pole placement of the uncorrected slow subsystem.

For the corrected solution,

$$\dot{x} = (A - BG_c)x \tag{3.15}$$

where Gc is the gain calculated from pole placement of the corrected slow subsystem.

CHAPTER 4

SIMULATION

Figures 4-1 to 4-6 show plots of the pitch angle vs. time that stability is maintained with an initial value of 1 rad applied. Figures 4-1 and 4-2 show the exact solution of pole placement. As expected, dampening takes place within a shorter interval for the exact solution compared to the uncorrected and corrected ones.

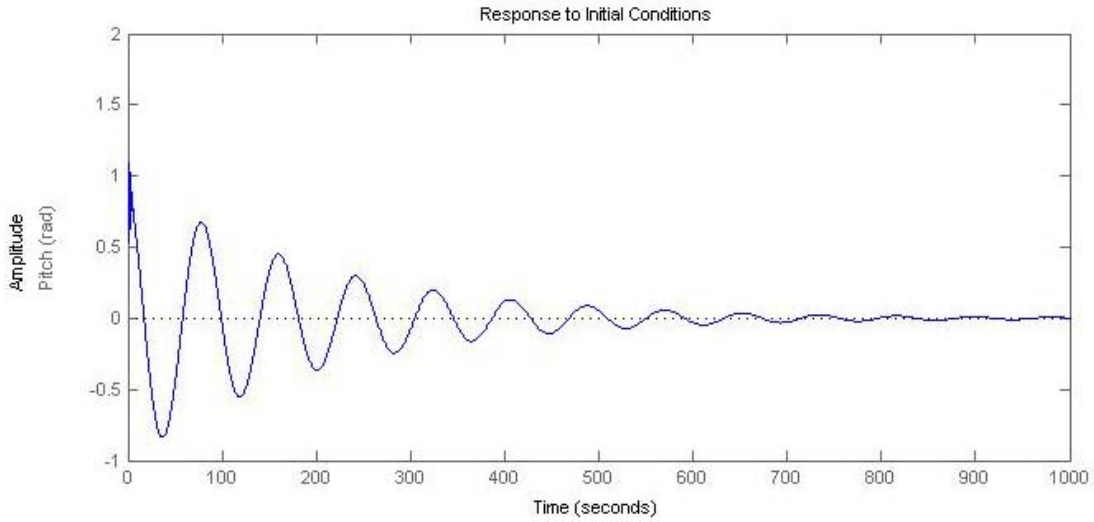

Figure 4-1. Exact Solution at -0.0050.

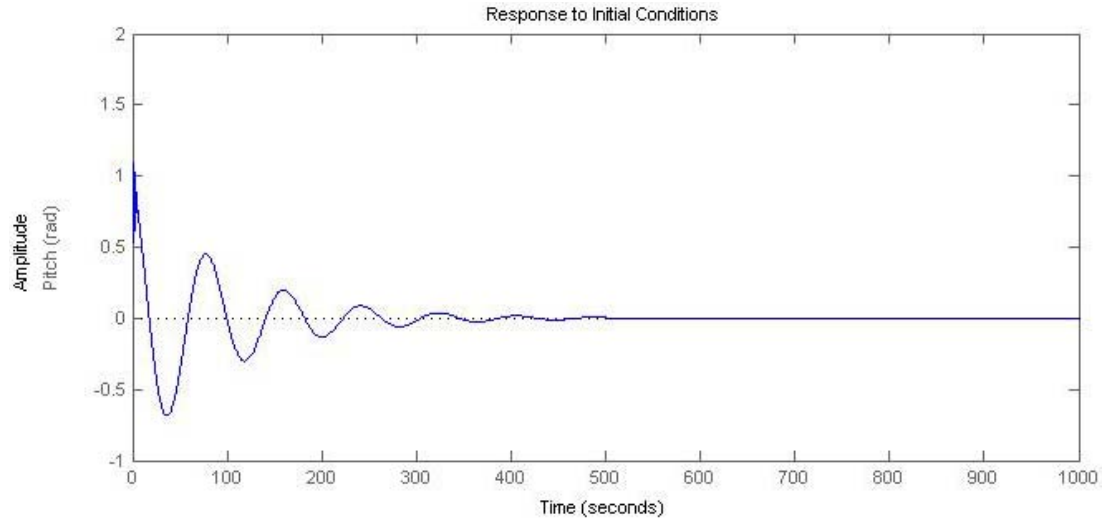

Figure 4-2. Exact Solution at -0.0100.

Figures 4-3 through 4-6 show the uncorrected and corrected solutions, respectively. Even though the plots show dampening taking approximately 10,000 seconds, the purpose of using this method is fulfilled because it provides a reduced-effort calculation on a system to ensure that stability still holds.

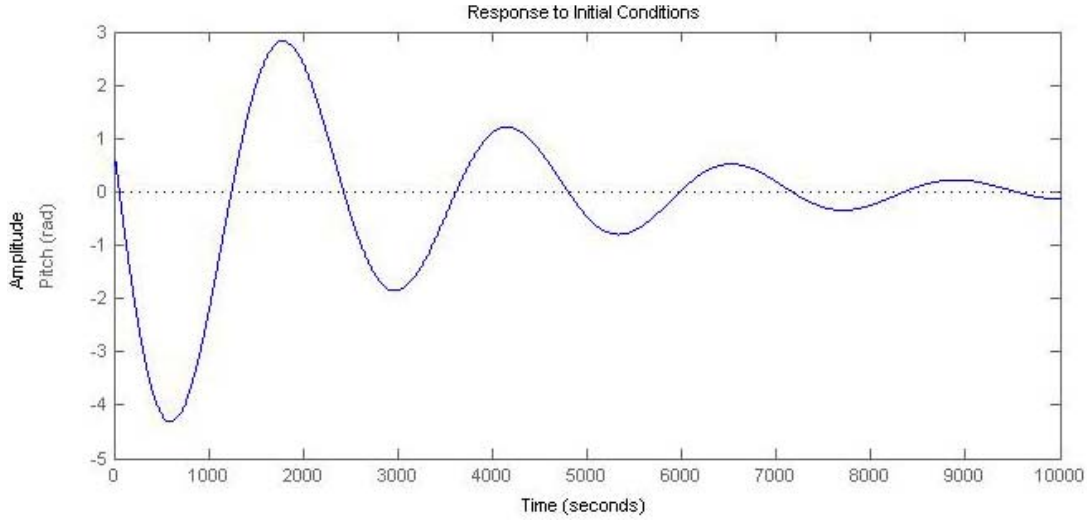

Figure 4-3. Uncorrected Solution at -0.0050.

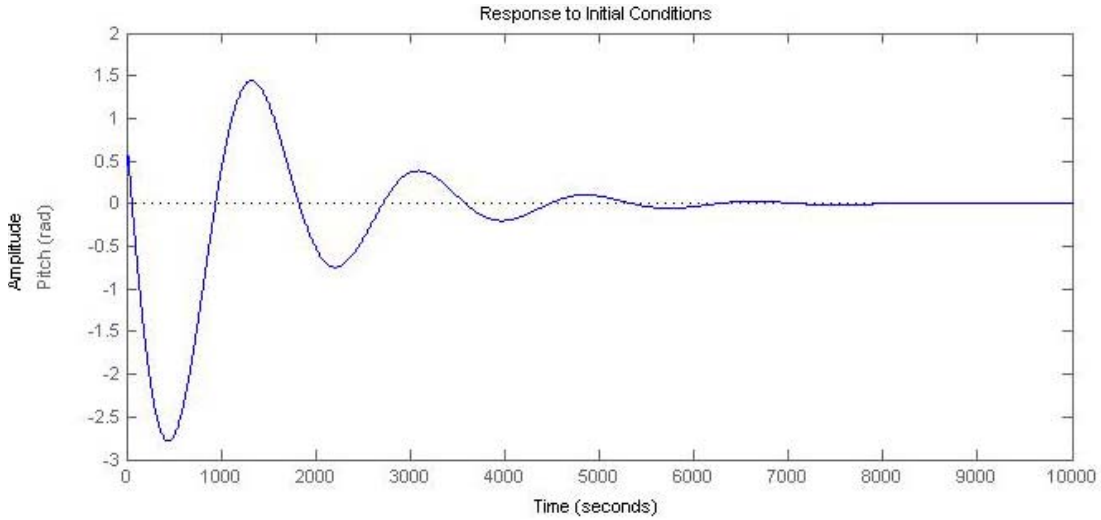

Figure 4-4. Uncorrected Solution at -0.0100.

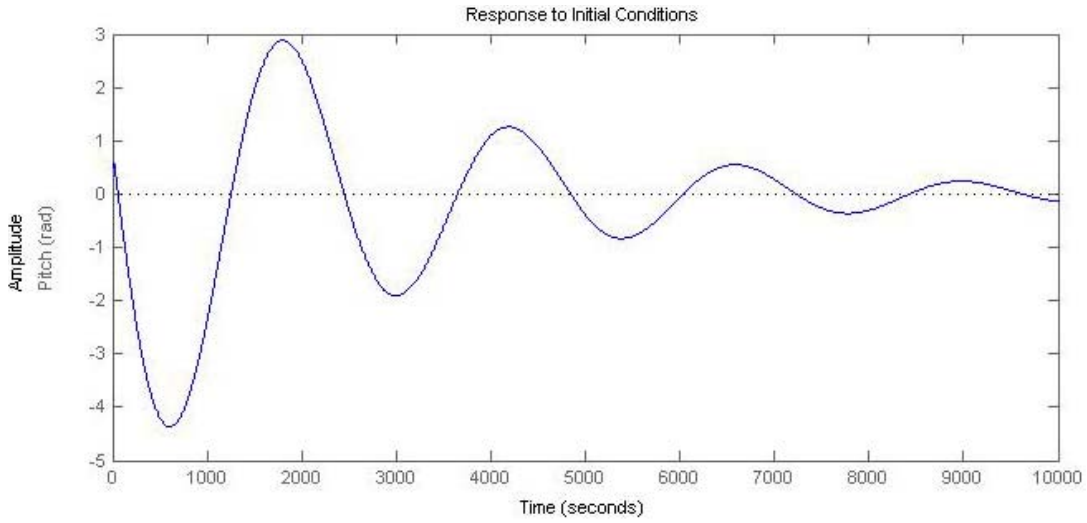

Figure 4-5. Corrected Solution at -0.0050.

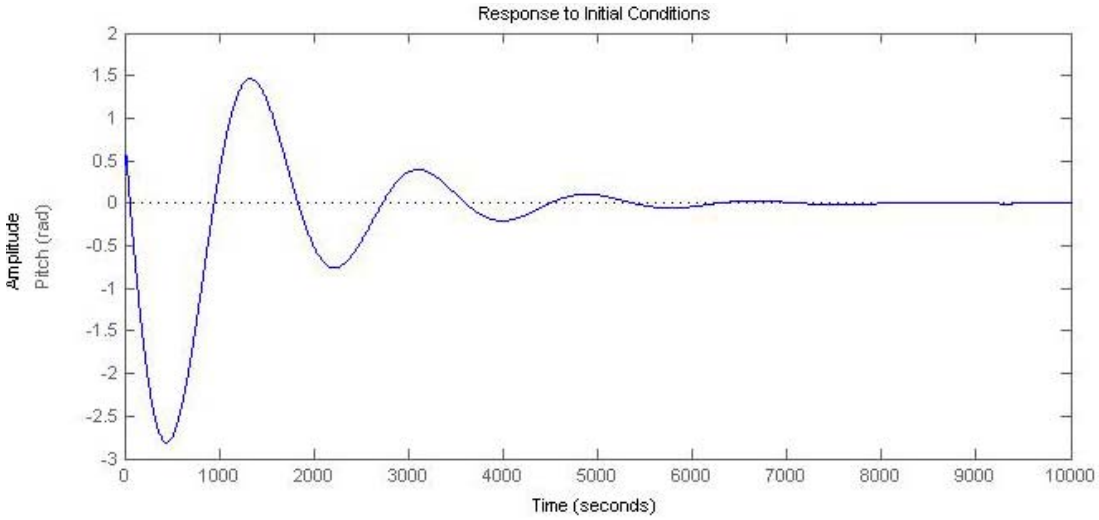

Figure 4-6. Corrected Solution at -0.0100.

The eigenvalues of the closed loop system for the pole placement at -0.0050 were as follows:

Exact Solution:

$$-0.665600000000000 \pm 2.182100000000002i$$

$$-0.005000000000000 \pm 0.076500000000000i$$

Uncorrected Solution:

-0.672222100746381 ± 2.179609446694929i

-0.000355726898124 ± 0.002648928211817i

Corrected Solution:

-0.672231293434171 ± 2.179584385361726i

-0.000346533107418 ± 0.002625341704260i

The deltas between the Exact system and Uncorrected system are as follows:

Fast Pole = 0.007086

Slow Pole = 0.073996

The deltas between the Exact system and Corrected system are as follows:

Fast Pole = 0.007083

Slow Pole = 0.074021

For the pole placement at -0.0100:

Exact Solution:

-0.665600000000000 ± 2.182100000000000i

-0.010000000000000 ± 0.076500000000000i

Uncorrected Solution:

-0.671831907570681 ± 2.180672686691589i

-0.000745960237997 ± 0.003554477175555i

Corrected Solution:

-0.671841085832996 ± 2.180647654348610i

-0.000736781007068 ± 0.003536576702767i

The deltas between the Exact system and Uncorrected system are as follows:

Fast Pole = 0.006557

Slow Pole = 0.073531

The deltas between the Exact system and Corrected system are as follows:

Fast Pole = 0.006408

Slow Pole = 0.073549

With an ε value of 0.0336, it can be seen from these results that the fast pole positions remain within O(ε) of the exact system, but the slow pole positions do not. In addition, no corrected solutions are within $O(\varepsilon^2)$. To account for this compared to the results of the Shim and Sawan paper, further analysis of the Simulink modeling used in that study compared to the MATLAB calculations used in this thesis need to be explored. In addition, more realistic pole relocation choices may be beneficial, but are outside the scope of this study.

4. SIMULATION

4.1 Stochastic Condition

As demonstrated in the previous section, the system maintains stability at the arbitrary selected slow pole values. Therefore, regarding stochastic conditions, it follows from this stability that a finite solution exists for the Lyapunov equation and the resulting covariance matrix is a positive definite one. As a data point exercise to confirm this, the solution to the Lyapunov equation was calculated for the -0.0050 pole location to obtain the covariance matrix as follows. [10]:

$$PA^T + AP + Q = 0 \tag{4.1}$$

where

$$Q = FQF^T \tag{4.2}$$

$$F = F_1 - A_{12}A_{22}^{-1}F_2 \tag{4.3}$$

$$F_1 = \begin{bmatrix} -0.223371 * 10^{-2} \\ 0 \end{bmatrix} \tag{4.4}$$

$$F_2 = \begin{bmatrix} -0.279448 * 10^{-2} \\ -1.596845 * 10^{-2} \end{bmatrix} \tag{4.5}$$

For this exercise, a wind disturbance was applied to the nose angle of attack and modeled as a Gaussian white noise with intensity Q [3]:

$$Q = \frac{\sigma^2 I}{\pi V_0^3} = 7.51273 * \ 10^{-4} \tag{4.6}$$

This yielded the positive definite covariance matrix

$$\begin{bmatrix} 4.5646 * 10^{-10} & -1.9387 * 10^{-26} \\ -1.9387 * 10^{-26} & 9.9750 * 10^{-10} \end{bmatrix} \tag{4.7}$$

CHAPTER 5

CONCLUSION AND FUTURE WORK

This thesis focused on the application of the quasi-steady-state approximation and matrix block diagonalization method utilized in the work of Shim and Sawan [1]. The technique was applied to the NASA F-8 digital fly-by-wire aircraft longitudinal dynamics. This particular aircraft model was chosen due to its well-documented characteristics and availability of data, which allowed validation of the stability results and stochastic data. It was demonstrated that once a system is transformed using the singular perturbation method into a two-time-scale form, an approximate solution can be obtained by only relocating the slow poles. This can be seen in the results of the corrected and uncorrected solutions. Although the dampening time is considerably longer than the original system and bounding within O(ε) was not entirely achieved, this method still shows that stability characteristics can still be determined. By successfully applying this technique to the NASA F-8 aircraft, it has been shown that this technique is not unique to the de Haviland Canada DHC-2 Beaver aircraft. Approximate solutions can be determined for other models along with the validation of maintaining stability and robustness during stochastic disturbances.

Future work in this area could be the continued validation of these techniques as they apply to other aircraft models. The author's intent is to further verify this technique at his place of employment, where he is involved in the flight test program of a new business jet. Here, models and data from various flight test phases and environmental conditions could be used to confirm if the system behavior of previous design changes

are predictable with acceptable accuracy using the approximation techniques in this thesis.

Although this paper focused on aircraft systems to employ these techniques, they would be applicable to any modeled dynamic system. This option for future work would demonstrate the universal application of these processes and further prove their versatility and usefulness.

REFERENCES

REFERENCES

[1] Shim, Kyu-Hong, and Sawan, M.E., 2005, “Approximate controller design for singularly perturbed aircraft systems,” *Aircraft Engineering and Aerospace Technology: An International Journal*, 77/4, pp. 311–316.

[2] Chang, K.W., 1974, “Diagonalization method for a vector boundary problem of singular perturbation type,” *Journal of Mathematical Analysis and Application*, 48, pp. 652–655.

[3] Mahmoud, M.S., and Chen, Y., 1983, “Design of feedback controllers by two-time-stage methods,” *Applied Mathematical Modelling*, 7, pp. 163–168.

[4] Kokotovic, Peter V., 1975, “A Riccati equation for block diagonalization of ill-conditioned systems,” *IEEE Trans. on Automatic Control*, 20, pp. 812–814.

[5] Chow, J., and Kokotovic, P.V., 1976, “Eigenvalue placement in two-time-scale systems,” paper presented at the IFAC Symposium on Large Scale Systems, pp. 321–326.

[6] Kokotovic, P.V., Khalil, H., and O’Reilly, J., 1986, *Singular Perturbation Methods in Control Analysis and Design*, Academic Press, Orlando, FL.

[7] Vian, J.L., and Sawan, M.E., 1994, "H_∞ control for a singularly perturbed aircraft model,” *Optimal Control Applications Applications & Methods*, 15, pp 277–289.

[8] Rauw, M., 1998, “FDC 1.2 – A SIMULINK Toolbox for Flight Dynamics and Control Analysis,” Dutchroll Software, The Netherlands.

[9] Elliot, J.R., 1977, "NASA's advanced control law program for the F-8 digital fly-by-wire aircraft," *IEEE Transactions on Automatic Control*, AC-22, No. 5, pp. 753–757.

[10] Stengel, Robert, F., 1986, *Stochastic Optimal Control, Theory and Application*, John Wiley & Sons, New York.